

High-energy ion-beam-induced phase separation in SiO_x films

W. M. Arnoldbik, N. Tomozeiu, E. D. van Hattum, R. W. Lof, A. M. Vredenberg, and F. H. P. M. Habraken
Surfaces, Interfaces and Devices, Debye Institute, Utrecht University, P.O. Box 80.000, 3508 TA Utrecht, The Netherlands
 (Received 6 July 2004; revised manuscript received 3 December 2004; published 28 March 2005)

The modification of the nanostructure of silicon suboxide (SiO_x) films as a result of high-energy heavy-ion irradiation has been studied for the entire range $0.1 \leq x < 2$. The SiO_x films have been obtained by radio-frequency magnetron sputter deposition. For 50 MeV ⁶³Cu⁸⁺ ions and an angle of incidence of 20° with the plane of the surface, and for $x \geq 0.5$, it takes a fluence of about $10^{14}/\text{cm}^2$ to reach a Si-O-Si infrared absorption spectrum, which is supposed to be characteristic for a Si-SiO₂ composite film structure. For smaller x values, it takes a much larger fluence. The interpretation of the IR spectra is corroborated for the surface region by results from x-ray photoelectron spectroscopy. The results present evidence for a mechanism, in which the phase separation takes place in the thermal spike, initiated by the energy deposited in many overlapping independent ion tracks. Such a process is possible since the suboxides fulfill the conditions for spinodal decomposition.

DOI: 10.1103/PhysRevB.71.125329

PACS number(s): 61.80.Jh, 64.75.+g, 68.65.-k, 61.43.Dg

INTRODUCTION

Silicon suboxide (SiO_x) is an interesting material. Its most promising application is as precursor material for Si nanometer sized clusters in a SiO₂ matrix, which are considered for application in optoelectronics.¹ An important aspect of SiO_x as a continuous random bonding network, with a statistical distribution of the number of O atoms on the corners of the tetrahedra with a Si atom as the central atom, is its instability, i.e., it has a strong tendency to separate in two phases Si and SiO₂. The phase separation has been reported to occur as a result of several kinds of activation: annealing,^{2,3} rapid thermal heating, Ar-plasma treatment and UV laser irradiation,⁴ swift heavy ion irradiation,⁵ and white synchrotron radiation.⁶ Recently, it has been shown to occur during deposition by evaporation of SiO (Ref. 6) and by magnetron plasma sputtering⁷ for a wide range of x as well. This seemingly intrinsic property of SiO_x to separate into the two phases Si and SiO₂ has been attributed to the penalty energies of the Si atoms with intermediate valence,^{6,8-10} which supposedly causes the Si-O system to fulfill the conditions for spinodal decomposition.^{7,11,12}

In this paper, we report the occurrence of phase separation in SiO_x layers for a wide range of suboxide composition ($0.1 \leq x < 2$) as a result of heavy ion irradiation, for a wide range of ion fluence [$10^{12} - (3 \times 10^{15})$ ions/cm²] in the energy range where the energy deposition in the solids through electronic stopping dominates (~ 1 MeV/a.m.u.). In these experiments, every ion deposits energy in a track along its path in the material, resulting a.o. in a sudden temperature rise (melting) and fast cooling of the material within a cylinder with radius of a few (2–15) nm: the “thermal spike.” The relevant lifetime of such a thermal spike is in the order of 10^{-10} s.¹³ With a typical particle current density of $10^{11}/(\text{cm}^2 \text{ s})$, we can consider every ion impact and concomitant ion track occurrence as one individual event in which a cylindrical piece of material is heated and quenched with a very high rate. A consequence is that the macroscopic temperature of the sample remains low, say 150 °C. At this

temperature, no changes of the material are noted during an anneal with a length of the experiment. This offers the possibility to obtain a Si-SiO₂ composite film at low temperature, but also to investigate the mechanism of the phase separation which is not straightforwardly studied using anneal treatments.³¹

EXPERIMENT

The SiO_x layers were obtained by rf magnetron sputtering of Si in an Ar/O₂ mixture onto a *c*-Si substrate, dipped in HF before deposition. Details of the deposition are given in Ref. 14. Our SiO_x films contain 2–4 at. % Ar with highest values in the lower x range.⁷ Also hydrogen is found in the films in Si-H bonding configuration in an amount of 1–4 at. %. We irradiated samples with $0.1 < x < 2$. Since SiO₂ and SiO_x layers are significantly thinned by electronic sputtering during irradiation and elemental *a*-Si is not,¹⁵ some of the SiO_x layers, to be characterized by Fourier transform infrared absorption spectroscopy, were covered by an *a*-Si film in the same deposition system. The thickness of the films amounted to 100 nm. We irradiated the SiO_x films at various fluences between $10^{12}/\text{cm}^2$ and $3 \times 10^{15}/\text{cm}^2$ with 50 MeV Cu⁸⁺ ions, from the Utrecht University 6.5 MV tandem accelerator, at an angle 20° with the plane of the surface, unless otherwise indicated. The particle current density amounted to about $2 \times 10^{11}/(\text{cm}^2 \text{ s})$. The stopping power of these ions at the surface of these materials is in the order of 8 keV/nm, the highest value applicable for $x=0$ and the lowest value for $x=2$. Only about 0.35% is to be ascribed to the nuclear energy loss.

The samples were investigated before and after irradiation with Fourier absorption infrared spectroscopy (FTIR), x-ray photoelectron spectroscopy (XPS), Raman spectroscopy, and Rutherford backscattering spectrometry (RBS) in combination with channeling. The samples for FTIR were irradiated in a system, containing an ionization chamber for simultaneous analysis using elastic recoil detection (ERD). The accuracy in the x values, as determined by combined RBS/

ERD analyses, amounts to less than 5%. The samples were transferred through air to a Digilab FTS-40 FTIR spectrometer equipped with an LN₂ cooled HgCdTe detector. The IR spectra were taken in transmission mode at a nonperpendicular angle of incidence of 25° with the surface normal using unpolarized light. XPS is mainly sensitive for the surface and therefore the irradiation of the samples for XPS analyses was performed in the UHV XPS chamber. In XPS, we used unmonochromatized Mg K_α radiation. The photoelectrons were detected at an angle of 78° with the surface normal in a CLAM100 hemispherical analyzer at a pass energy of 20 eV. Both irradiation systems were connected to the Utrecht 6.5 MeV EN tandem accelerator.

The samples, having dimensions of about 10 × 10 mm, were clamped mechanically on a stainless steel base plate. During the irradiation the macroscopic temperature of the sample remained below 150 °C, as deduced from a temperature indicator¹⁶ with a very small heat capacity, which was attached on the sample surface close to the spot where the ion beam hits the sample. To increase the homogeneity of the irradiation over the beam spot on the sample, the ion beam was defocused and collimated, resulting in a beam spot of approximately 3 × 3 mm, significantly larger than the probed area in infrared spectroscopy and XPS (~1 × 1 mm). We estimate the absolute accuracy of the fluence to be about 30%, and the relative accuracy to be below 10%. In the first few seconds of the 50 MeV Cu⁸⁺ irradiation, almost all Ar desorbs from the films as measured with a rest gas analyzer during irradiation and Rutherford backscattering spectrometry (RBS) after the irradiation. In contrast, during the 2 MeV He irradiation in the RBS analyses, Ar remained in the films.

RESULTS AND DISCUSSION

IR analysis

The vibrational spectrum of SiO₂ is full of details and is well-documented.^{18,19} It consists of longitudinal optical–transverse optical (LO–TO) split features at around 460 cm⁻¹, 800 cm⁻¹, and 1100 cm⁻¹. The LO modes are not detected (lower frequencies) or only detected in oblique incidence IR transmission measurements. The highest-frequency feature exhibits the largest absorption coefficient, therefore in the literature most attention is paid to this absorption band. In SiO₂ it features a TO absorption peak at around 1070 cm⁻¹ with a LO absorption at around 1250 cm⁻¹, being visible applying oblique incident IR radiation.

As is usually done, in the present work we focus on the region of the Si–O–Si stretching mode (750–1400 cm⁻¹). At first we present the IR spectra of thermally grown and our rf sputtered SiO₂ films, with and without irradiation (Fig. 1). Below, we summarize briefly the assignment of the relevant regions as described in the literature. Similar (i.e., nonperpendicularly taken) IR spectra of SiO₂ films have been presented and discussed in Ref. 17. Here, the peak at around 1080 cm⁻¹ is interpreted to originate from the in-phase asymmetric Si–O–Si stretching TO (TO₃) mode of bridging oxygen in SiO₂. The absorption at 1256 cm⁻¹ in the SiO₂

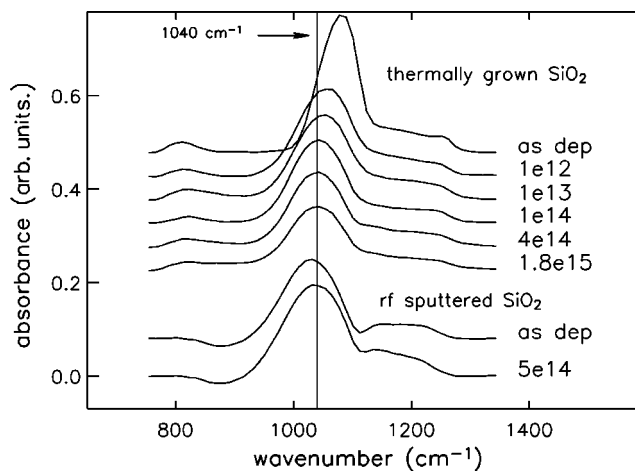


FIG. 1. IR absorption spectra of thermally grown and rf sputtered SiO₂ films before and after irradiation with 50 MeV Cu ions for the various fluences (ions/cm²) as indicated.

films is visible in IR analyses with a nonperpendicularly incident IR beam as is the case here, and is a LO (LO₃) splitting of the 1080 cm⁻¹ TO₃ mode. The origin of the feature at around 1150–1200 cm⁻¹ is still controversial:¹⁸ it is associated with a fourth, but inverted in energy, LO–TO split mode (TO₄–LO₄), induced by disorder in the microstructure^{17,19} and/or with porosity as in SiO₂ sol-gel derived silica films.²⁰ These assignments have led authors to draw conclusions about the microstructure of their oxide films from the relative intensity of this fourth mode, as compared to the TO₃ mode absorption intensity.²¹

The unirradiated thermally grown oxide shows the TO₃ peak at 1080 cm⁻¹ as expected (Fig. 1). However, in our rf sputtered SiO₂ layers, i.e., layers with a RBS determined stoichiometry of SiO₂ and no measurable Siⁿ⁺ ($n < 4$) concentration as determined with XPS, the TO₃ absorption peaks in the region 1040–1060 cm⁻¹ before irradiation.¹⁵ A peak position of 1040 cm⁻¹ for the asymmetric Si–O–Si stretching vibration absorption has been reported earlier for low-temperature grown SiO₂.²² This position of the TO₃ peak can also be obtained by ion irradiation. Awazu *et al.*²³ report that the IR asymmetric Si–O–Si TO₃ absorption mode in thermally grown SiO₂ layers shifts from 1078 down to 1044 cm⁻¹, with a concomitant shift of the 1200 cm⁻¹ feature, as a result of ion irradiation with many different MeV ion beams. This shift is reversed during annealing at 600 °C and is ascribed to a structural modification in the SiO₂. Figure 1 shows that this shift to lower wave numbers was reproduced in our irradiation conditions. The area ratio TO₄/TO₃ does not seem to be strongly influenced by the irradiation.²³ It seems that similar structural damage is present in our as-deposited SiO₂ layers as in the irradiated thermally grown oxides, presumably due to the ion bombardment during the plasma deposition or to the low temperature during growth. Consistently, we do not note a significant shift of the peak as a result of irradiation of the rf sputtered oxides with 50 MeV Cu ions to a fluence of 5×10^{14} /cm².

The TO₃ mode is positioned at smaller wave numbers in substoichiometric silicon oxide layers.²⁴ Figure 2(a) shows

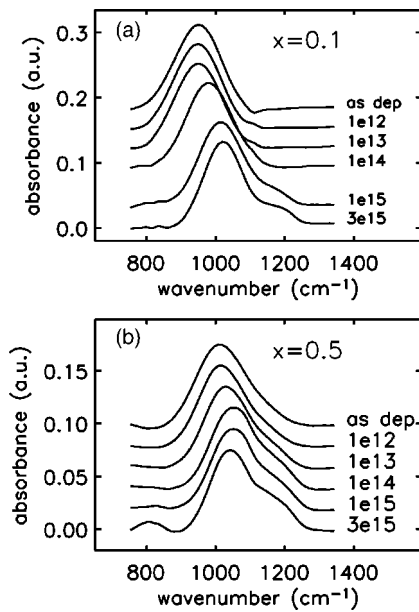


FIG. 2. IR absorption spectra of SiO_x films, before and after irradiation with 50 MeV Cu ions for the fluences (ions/cm²) as indicated. (a) $x=0.1$, (b) $x=0.5$.

the background corrected absorbance in the region of the Si-O-Si asymmetric stretching vibration for the $\text{SiO}_{0.1}$ film of $\sim 1 \mu\text{m}$ thickness for a wide range of ion fluences. In the as-deposited film, the peak maximum appears at 952 cm^{-1} . Irradiation with a fluence of $1 \times 10^{13}/\text{cm}^2$ or lower does not influence this peak position, but for higher fluences the peak maximum shifts to higher wave numbers up to 1024 cm^{-1} for the highest fluence of $3 \times 10^{15}/\text{cm}^2$ applied. During irradiation, the O concentration does not vary, as we have verified using simultaneous ERD measurements. From the combined IR and ERD result, it is clear that the Si-O-Si peak position is not a good measure for the average suboxide stoichiometry. In contrast, the combination of the two methods, owing to the induction effect that causes the shift of the IR vibrational modes,²⁵ leads us to conclude that the oxygen atoms to an increasing extent become located in oxygen-rich regions, at the expense of oxygen-poor regions (disproportionation). Interestingly, at the higher fluences also a feature very well attributable to the TO_4 mode becomes visible.

Figure 2(b) shows a similar sequence of IR spectra of SiO_x films for $x=0.5$. Also for this sample we find a shift to higher wave numbers as a result of irradiation up to 1×10^{15} Cu ions per cm^2 . Apart from the higher wave numbers for this sample, we note three other differences as compared to the $x=0.1$ sample. At first we already note a shift of the peak absorbance for an irradiation at a fluence as low as $1 \times 10^{13}/\text{cm}^2$. Secondly, the relative contribution of the TO_4 mode is already visible after a fluence of $1 \times 10^{12}/\text{cm}^2$ and its contribution to the total absorption is much larger than for the $x=0.1$ sample. Thirdly, in the high fluence range the TO_3 peak position tends to shift to lower wave numbers, from the maximum value of about 1050 cm^{-1} down to about 1042 cm^{-1} . An important observation is that in none of the suboxide samples do we find a significant change of the TO_3 absorption full width at half maximum peak width with irradiation fluence.

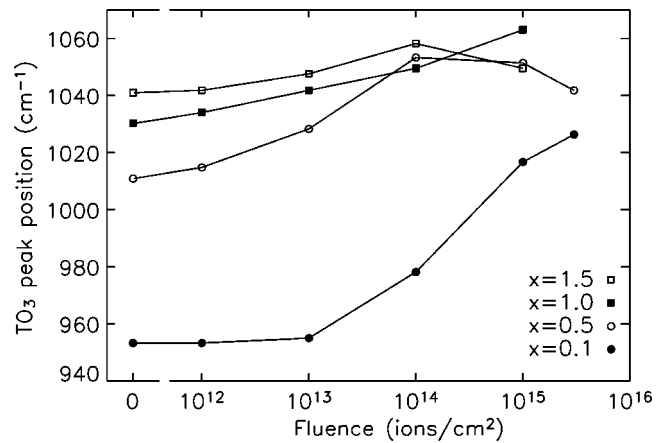


FIG. 3. Evolution of the IR TO_3 absorption peak maximum as a function of 50 MeV ion fluence for the various suboxides, as indicated.

The positions at maximum absorbance as a function of fluence are presented in Fig. 3 for the various x values in SiO_x . All samples show an upward shift upon irradiation, but around a fluence of 10^{14} – $10^{15}/\text{cm}^2$ a saturation sets in (except for $x=0.1$) or, stated probably more appropriately, when the peak value amounts to about 1045 cm^{-1} . For larger fluences in some samples the peak position seems to decrease and in others it appears to increase, indicative of the complexity of the process at high fluence, which is larger than assumed here.¹⁰

Using the results of Ref. 23 and those given in Fig. 1, the transition from 1076 cm^{-1} down to 1044 cm^{-1} as a result of ion irradiation of high-temperature SiO_2 is estimated to be completed under our conditions around a fluence of 10^{12} – 10^{13} ions/cm², i.e., in the early stages of our irradiations. Since the observed peak positions in the IR spectra reach this value of 1044 cm^{-1} , we conclude that for all x values, except $x=0.1$, after irradiation with fluences of $10^{14}/\text{cm}^2$ and larger, the O is incorporated in an SiO_2 -type environment. Since the overall O concentration does not change during irradiation, simultaneously oxygen-free regions must have been formed: phase separation. On the other hand, the spectra do not resemble those of the oxide films (Fig. 1), in view of the absence of the 1256 cm^{-1} LO_3 mode and the relatively large contribution of the TO_4 mode. In fact, the spectra resemble those of SiO_2 in SiO_2 -Ge (Ref. 26) and SiO_2 -SiC (Ref. 27) composite films. Similarly, Hayashi *et al.*²⁸ have found similar TO_4/TO_3 ratios for 2-nm-thick SiO_2 layers covering 10 nm Si particles. This all leads us to conclude that our swift heavy-ion irradiated films are very well considered to be a Si- SiO_2 composite material, with, however, small, ion beam damaged SiO_2 regions. It is presumed that also the $x=0.1$ film will reach this stage after prolonged irradiation.

In our conditions, the shift of the TO_3 peak saturates at a fluence of about 10^{14} – $10^{15}/\text{cm}^2$. This is in apparent contrast to the saturation reported to occur at a fluence of about $10^{12}/\text{cm}^2$ for irradiation of SiO_1 with 863 MeV Pb ions,⁵ even more so since we apply a (glancing) angle of 20° which is to be contrasted with the perpendicular incidence in Ref. 5. This difference probably is due to the factor of 2–3 smaller

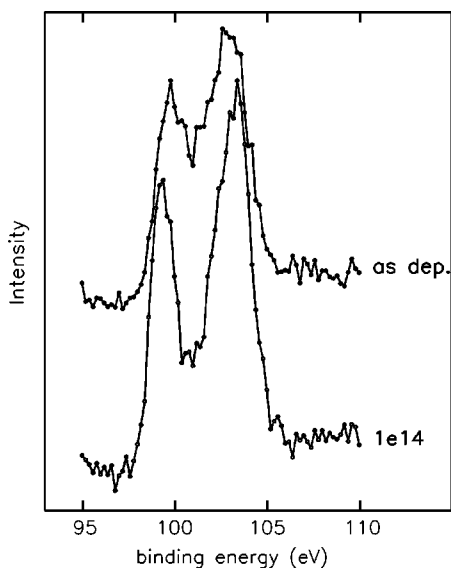


FIG. 4. Si(2*p*) XPS spectra of SiO_{0.7} before and after irradiation with 50 MeV Cu ions for a fluence of 10¹⁴ ions/cm².

stopping power of our 50 MeV Cu ions in comparison to that of the 863 MeV Pb ions (24.5 keV/nm).

In order to find out whether the silicon in the irradiated SiO_{*x*} films is possibly present in crystalline form, SiO_{*x*} films with the *x* values 0.1, 0.5, 1.0, and 1.5 were grown on Corning glass and irradiated under the same conditions. These films were inspected using Raman spectroscopy. A contribution at 520 cm⁻¹ of the TO mode of crystalline silicon could not be discovered in the Raman spectrum at ion fluences up to 3 × 10¹⁵ ions/cm². This indicates that the Si nanocrystals, if present at all, have a size smaller than 2 nm.²⁹

XPS

XPS analyses have been performed on noncapped SiO_{*x*} films. Irradiation under the conditions of this paper results in thinning of the SiO_{*x*} film by electronic sputtering. The initial O removal rate strongly depends on the suboxide composition and on the angle of incidence^{15,30} and can be as large as ~10³ (Ref. 15) atoms removed for SiO₂ and a glancing angle of incidence of 6°. Also here, the O bulk concentration remains constant during irradiation, as deduced from the height of the O ERD feature.

Figure 4 presents the Si(2*p*) XPS spectral region of SiO_{0.7} sample before and after a fluence of 10¹⁴ ions/cm². The Si(2*p*) photoelectron peak was deconvoluted with the usual procedure into the components corresponding to five distinct nearest-neighbor surroundings of the Si atoms with zero, one, two, three or four O atoms.^{6,7} The photoelectron spectrum of Fig. 4 appears indicative for the random-bonding network with a preferential occurrence of Si(Si₄) and Si(O₄) tetrahedral units of these as-deposited SiO_{*x*} samples.⁷ As a result of ion irradiation, the high-energy side of the Si(2*p*) photoelectron feature shifts to higher binding energy, towards a binding energy, usually found in SiO₂. Concomitantly, the low-energy side shifts to lower energy and a clear peak arises, at an energy usually found for elemental silicon.

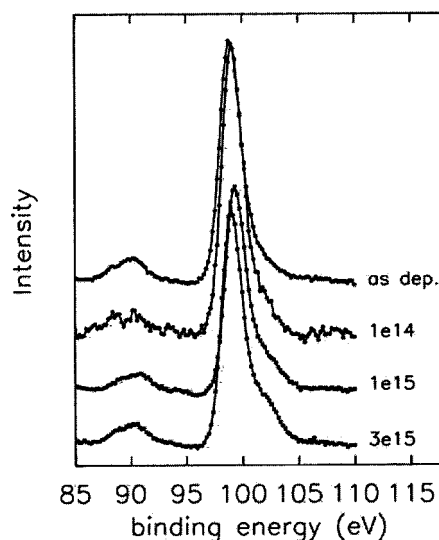


FIG. 5. Si(2*p*) XPS spectra of SiO_{0.1} before and after irradiation with 50 MeV Cu ions for the fluences (ions/cm²) as indicated.

This behavior of the Si(2*p*) photoelectron peak is again a clear indication for phase separation in the suboxide, but now for the surface region. The deconvolution of the photoelectron peak in the distinct SiO_{*n*} building blocks shows that the concentrations of Si¹⁺, Si²⁺, and Si³⁺ in the surface region diminish during irradiation, to the benefit of the Si⁰ and, initially, of the Si⁴⁺ concentration: Here, it is important to bring forward that ERD measurements and also RBS/channeling measurements indicate that the layers are not so thinned by sputtering that the increase of the Si⁰ concentration can be ascribed to the vicinity of the *c*-Si substrate.

Figure 5 shows the Si(2*p*) XPS spectral region for the sample with *x*=0.1. We note a development of the shoulder at the high-energy side only for fluences larger than 10¹⁴/cm², in agreement with the findings using IR. Also, in agreement with the IR data we deduce from the peak shape that after the highest fluence of 3 × 10¹⁵ ions/cm² the spectrum does not resemble that of a Si-SiO₂ phase-separated mixture.

Mechanism

The experimental data convincingly show that irradiation of SiO_{*x*} with 50 MeV Cu ions results in the formation of oxygen-rich and oxygen-poor regions in the films. The observations are consistent with the inference that for prolonged irradiation the oxygen-rich regions consist in fact of SiO₂, albeit a damaged or low-temperature form of SiO₂. The oxygen-poor regions may very well be oxygen-free regions in view of the observation that the IR absorption at around 950 cm⁻¹, characteristic for a SiO_{*x*} film with a low value of *x*, disappears.

This observation of phase separation in SiO_{*x*} as a result of ion beam irradiation is completely in line with the well known phenomenon that thermal annealing of silicon suboxides (with or without hydrogen incorporated) above a temperature of 700 °C results in (crystalline) Si and SiO₂ phase separation,^{2,3,31,32} indicating that the phase-separated mixture

is a more stable configuration than an amorphous silicon suboxide random bonding network and thus has a lower free energy. In fact, the shift of the IR absorption peak maximum behaves as a function of irradiation fluence in a similar manner as the shift of this maximum as a function of annealing time³¹ when we emphasize the deceleratory behavior of the peak shift with ion fluence. This behavior appears not straightforwardly described with a nucleation and growth model and therefore does not support such a model.³¹ An argument against nucleation and growth of SiO₂ regions deduced from the present measurements is that we do not observe an increase in the widths of the distinct IR absorption features, which would be indicative of a change of the inhomogeneity in the O bonding environments. Especially we do not observe features at intermediate stages of irradiation, which we could ascribe to the existence of SiO₂ regions in a more oxygen-poor matrix. Within the view of spinodal decomposition, the observed phase separation during irradiation proceeds in a large number of small steps, in which oxygen-rich regions in the material gradually become more oxygen-rich and oxygen-poor regions become more oxygen-poor. This process requires mobility of atoms in the solid. The activation for the mobility of the atoms involved is, of course, delivered by the ion impact in the process of, predominantly, electronic stopping. It is generally accepted that in this stopping regime energy is transferred from the high-energy ion into the electronic system of the solid by excitation and ionization within a cylindrical region along the straight ion path: the Coulombic ion track. In metals and semiconductors, the lifetime of this positively charged ion track is supposed to be so small that the repulsive force does not cause a significant motion of the atoms. The energy stored in the electronic system is then transferred to the lattice, resulting in a large temperature rise along the ion path: the thermal spike.^{13,33} For insulators the situation is more controversial. It especially concerns the question if possibly the neutralization time of the charged track is long enough to set the ions into significant motion by the repulsive electrostatic force, such as proposed to take place in a Coulomb explosion,³⁴ or that another mechanism is responsible for transferring electronic energy into the lattice atom system, such as in exciton models.^{35,36}

The mentioned differences between metals/semiconductors and insulators become explicit when one looks to, e.g., the rate of electronic sputtering in SiO_x ($0 < x < 2$). SiO₂ is removed at a relatively high rate during MeV/a.m.u. ion impact on SiO₂, whereas Si is virtually not sputtered from a Si surface.¹⁵ Suboxides, which have intermediate electronic properties, show intermediate values for the sputter rate with a pronounced transition for $x \cong 1.2$.³⁰ On the basis of a.o. this argument we came to the conclusion that the rate-determining step in the electronic sputtering of SiO₂ is of an electronic nature.³⁷ We deduce from the electronic sputter behavior in the present work that we deal with films exhibiting metallic behavior (e.g., SiO_{0.1}) and with films with increasing insulating character with increasing x .

The current understanding of the phenomena associated with the passage of a swift ion through a solid, as presented above, helps us to understand the observation that for the SiO_{0.1} sample, the necessary fluence for phase separation to

occur is much larger than for the other samples. This lower rate of phase separation in SiO_{0.1} is also apparent in the intermediate stage where the local SiO_x structure resembles that of the other suboxides, i.e., where the IR peak maximum for the SiO_{0.1} sample is equal to that of the other samples (see Fig. 3). We ascribe this to a smaller lifetime of the Coulomb track and/or lower thermal spike temperature in the SiO_{0.1} in comparison to suboxides with larger O concentrations. Of course, the fact that, initially, in SiO_{0.1} the average distance for the O atoms to travel before dioxide regions can be formed, does also contribute to the lower initial rate of phase separation. Independent experimental evidence for the mobility of O in SiO₂ under irradiation has recently been found. In a study of the effects of 50 MeV Cu-ion irradiation of Si¹⁶O₂/Si¹⁸O₂ double layer structures, we indeed found isotope mixing at the oxide/oxide interface and desorption of O₂, deduced to escape from a region of the order of 5 nm below the surface.³⁸ The proposed mechanism is that O₂ molecules are produced in the entire ion track but most of these are trapped in the solid, when the distance to the surface is larger than a few nm. Formation of O₂ is the result of bond breaking in the ion track caused by the electronic excitation and ionization and a subsequent combination of two O atoms, occurring in competition with trapping to a Si atom.^{39,40} It is clear that also the process of O₂ formation requires some mobility of O atoms in the solid, like the process of phase separation, therefore there is no reason to suppose that O₂ molecule formation is a prerequisite for phase separation. Based on the aforementioned theoretical notions and experimental findings, it is expected that the modifications as a result of ion impact are a local effect, which results in an inhomogeneous material structure consisting of non-modified and cylindrical modified regions at fluences where only a part of the spot area has not been hit one or several times. Again, the absence of the broadening of the TO₃ IR absorption does not indicate a significant increase of the inhomogeneity of surroundings of the Si-O-Si bridges. Since this holds also for small fluences of 10¹²–10¹³/cm², a small modified volume and large modification per ion impact event are not consistent with the absence of broadening. The observed linearity of the shift of the IR absorption peak maximum with the logarithm of the fluence in relevant fluence ranges (Fig. 3) is not conceivable in a (simple) model in which a volume in the film has to be hit one time for a complete phase separation (Poisson distribution of nonhit volume). Consequently, we propose that the modified volume/ion is so large that even at the low fluences of 10¹²–10¹³/cm², most of the material has been influenced by several individual ion impact events. For instance, for $x=0.1$ the IR spectrum hardly changes for fluences of 10¹³/cm² and smaller. Even for a (hypothetical) track radius as small as 1 nm, 60% of the material volume in the beam spot has been part of an ion track at a fluence of 10¹³/cm²; for larger track radii, this volume fraction increases in a square fashion with this radius. So, for $x=0.1$ the modification per ion passage is certainly small. For larger x values, shifts in the IR spectra are already noted for fluences as small as 10¹²/cm² without a broadening of the peak, suggesting that the modification volume per ion impact is so large that at 10¹²/cm² the entire volume has been influenced several

times. So, we tend to conclude that the process of phase separation does not take place predominantly within the Coulombic track cylinder, which is supposed to have a radius of 1 nm or smaller. Similar conclusions have been drawn in Ref. 5.

The lifetime of a thermal spike following the ion passage in α -SiO₂ quartz has been calculated to be smaller than 10⁻¹⁰ s when one defines the spike to be terminated when the temperature drops below 1000 K. This figure in quartz is for a cylindrical region with a radius of about 14 nm around the ion trajectory. For smaller radii around the track, the track temperature is calculated to be much higher but the time at this temperature much shorter.¹³ For metallic samples, the temperature rise is expected to be lower. For a thermal spike radius of 10 nm, and 20° angle of incidence, the fluence to cover the entire surface once is in the order of 10¹¹/cm², i.e., one order of magnitude lower than the lowest fluence applied in this work.

Therefore, we consistently deduce that the MeV ion beam induced Si/SiO₂ phase separation takes place in the thermal spike initiated by the energy deposition from the swift ion

into the electronic system of the solid, in many small steps, in compliance with the process of spinodal decomposition and in agreement with the results of recent computations of Burakov *et al.*¹⁰ for silicon suboxides.

CONCLUSION

For all compositions 0.1 ≤ x < 2, radiofrequent magnetron sputtered silicon suboxide SiO_x films separate in the phases Si and SiO₂ as a result of swift heavy ion irradiation. For our conditions of 50 MeV ⁶³Cu⁸⁺ ions at an angle of incidence of 20° with the plane of the surface, and for x ≥ 0.5, it takes a fluence of about 10¹⁴/cm² to reach a stable IR Si-O-Si absorption feature, which is supposed to be characteristic for a Si-SiO₂ composite film structure. For smaller x values it takes a much larger fluence. The phase separation is proposed to take place, in distinct events, by the energy deposited by the individual swift heavy ions into a cylindrical volume of the solid around the ion path and in the thermal spike period after the ion passage, in compliance with the process of spinodal decomposition.

-
- ¹L. Pavesi, L. dal Negro, C. Mazzoleni, G. Franzo, and F. Priolo, *Nature* (London) **408**, 440 (2000).
- ²M. Hamasaki, T. Adachi, S. Wakayama, and M. Kikuchi, *J. Appl. Phys.* **49**, 3987 (1978).
- ³J. Ni and E. Arnold, *Appl. Phys. Lett.* **39**, 554 (1981).
- ⁴F. Rochet, G. Dufour, H. Roulet, B. Pelloie, J. Perrière, E. Fogarassy, A. Slaoui, and M. Froment, *Phys. Rev. B* **37**, 6468 (1988).
- ⁵D. Rodichev, Ph. Lavallard, E. Doryh e, A. Slaoui, J. Perrière, M. Gandais, and Y. Wang, *Nucl. Instrum. Methods Phys. Res. B* **107**, 259 (1996).
- ⁶A. Barranco, J. A. Mejias, J. P. Espin os, A. Caballero, A. R. Gonz alez-Elipe, and F. Yubero, *J. Vac. Sci. Technol. A* **19**, 136 (2001).
- ⁷J. J. van Hapert, A. M. Vredenberg, E. E. van Faassen, N. Tomozeiu, W. M. Arnoldbik, and F. H. P. M. Habraken, *Phys. Rev. B* **69**, 245202 (2004).
- ⁸D. R. Hamann, *Phys. Rev. B* **61**, 9899 (2000).
- ⁹A. Bongiorno and A. Pasquarello, *Phys. Rev. B* **62**, R16326 (2000).
- ¹⁰V. M. Burlakev, G. A. D. Briggs, A. P. Sutton, A. Bongiorno, and A. Pasquarello, *Phys. Rev. Lett.* **93**, 135501 (2004).
- ¹¹J. D. Gunton and M. Droz, *Introduction to the Theory of the Metastable and Unstable States*, Lecture Notes in Physics, Vol. 183 (Springer Verlag, Berlin, 1983).
- ¹²K. Binder, *J. Non-Equilib. Thermodyn.* **23**, 1 (1998).
- ¹³M. Toulemonde, Ch. Dufour, A. Meftah, and E. Paumier, *Nucl. Instrum. Methods Phys. Res. B* **166–167**, 903 (2000).
- ¹⁴N. Tomozeiu, E. E. van Faassen, W. M. Arnoldbik, A. M. Vredenberg, and F. H. P. M. Habraken, *Thin Solid Films* **420–421**, 382 (2002).
- ¹⁵W. M. Arnoldbik, N. Tomozeiu, and F. H. P. M. Habraken, *Nucl. Instrum. Methods Phys. Res. B* **190**, 433 (2002).
- ¹⁶Omegalabel, see <http://www.omega.com>.
- ¹⁷P. Lange and W. Windbracke, *Thin Solid Films* **174**, 159 (1989).
- ¹⁸P. Innocenzi, *J. Non-Cryst. Solids* **316**, 309 (2003).
- ¹⁹C. T. Kirk, *Phys. Rev. B* **38**, 1255 (1988).
- ²⁰R. M. Almeida and C. G. Pantano, *J. Appl. Phys.* **68**, 4225 (1990).
- ²¹A. Barranco, F. Yubero, J. P. Espin os, J. Ben itez, A. R. Gonz alez-Elipe, J. Cotrino, J. Allain, T. Girardeau, and J. P. Riviere, *Surf. Coat. Technol.* **142–144**, 856 (2001).
- ²²W. A. Pliskin and H. S. Lehman, *J. Electrochem. Soc.* **112**, 1015 (1965).
- ²³K. Awazu, S. Ishii, K. Shima, S. Roorda, and J. L. Brebner, *Phys. Rev. B* **62**, 3689 (2000).
- ²⁴P. G. Pai, S. S. Chao, Y. Takagi, and G. Lucovsky, *J. Vac. Sci. Technol. A* **4**, 689 (1986).
- ²⁵G. Lucovsky, J. Yang, S. S. Chao, J. E. Tyler, and W. Czubatj, *Phys. Rev. B* **28**, 3225 (1983).
- ²⁶M. Fujii, M. Wada, S. Hayashi, and K. Yamamoto, *Phys. Rev. B* **46**, 15 930 (1992).
- ²⁷Y. P. Guo, J. C. Zheng, A. T. S. Wee, C. H. A. Huan, K. Li, J. S. Pan, Z. C. Feng, and S. J. Chua, *Chem. Phys. Lett.* **339**, 319 (2001).
- ²⁸S. Hayashi, S. Tanimoto, and K. Yamamoto, *J. Appl. Phys.* **68**, 5300 (1990).
- ²⁹Z. Iqbal and S. Vepřek, *J. Phys. C* **15**, 377 (1982).
- ³⁰W. M. Arnoldbik, N. Tomozeiu, P. A. Zeijlmans van Emmichoven, and F. H. P. M. Habraken (unpublished).
- ³¹B. J. Hinds, F. Wang, D. M. Wolfe, C. L. Hinkle, and G. Lucovsky, *J. Vac. Sci. Technol. B* **16**, 2171 (1998).
- ³²E. San Andr es, A. del Prado, I. M artil, G. Gonz alez D iaz, F. L. Martinez, D. Bravo, and F. J. L opez, *Vacuum* **67**, 531 (2002).
- ³³E. M. Bringa and R. E. Johnson, *Phys. Rev. Lett.* **88**, 165501 (2002).
- ³⁴E. S. Parilis, in *Atomic Collisions on Solids*, edited by D. W. Palmer (North Holland, Amsterdam, 1970).

- ³⁵M. Sporn, G. Libiseller, T. Neidhart, M. Schmid, F. Aumayr, H. P. Winter, P. Varga, M. Grether, D. Niemann, and N. Stolterfoht, *Phys. Rev. Lett.* **79**, 945 (1997).
- ³⁶N. Itoh and A. M. Stoneham, *Nucl. Instrum. Methods Phys. Res. B* **146**, 362 (1998).
- ³⁷W. M. Arnoldbik, N. Tomozeiu, and F. H. P. M. Habraken, *Nucl. Instrum. Methods Phys. Res. B* **203**, 151 (2003).
- ³⁸W. M. Arnoldbik, N. Tomozeiu, and F. H. P. M. Habraken, *Nucl. Instrum. Methods Phys. Res. B* **219–220**, 312 (2004).
- ³⁹M. E. Adel, O. Amir, R. Kalish, and L. C. Feldman, *J. Appl. Phys.* **66**, 3248 (1989).
- ⁴⁰C. H. M. Marée, A. M. Vredenberg, and F. H. P. M. Habraken, *Mater. Chem. Phys.* **46**, 198 (1996).